Branching points in the low-temperature dipolar hard sphere fluid

Lorenzo Rovigatti, Sofia Kantorovich, Alexey O. Ivanov, José Maria Tavares, and Francesco Sciortino

Citation: J. Chem. Phys. **139**, 134901 (2013); doi: 10.1063/1.4821935
View online: http://dx.doi.org/10.1063/1.4821935
View Table of Contents: http://jcp.aip.org/resource/1/JCPSA6/v139/i13
Published by the AIP Publishing LLC.

Additional information on J. Chem. Phys.

Journal Homepage: http://jcp.aip.org/
Journal Information: http://jcp.aip.org/about/about_the_journal
Top downloads: http://jcp.aip.org/features/most_downloaded
Information for Authors: http://jcp.aip.org/authors

ADVERTISEMENT

Downloaded 01 Oct 2013 to 141.108.6.119. This article is copyrighted as indicated in the abstract. Reuse of AIP content is subject to the terms at: http://jcp.aip.org/about/rights_and_permissions

Branching points in the low-temperature dipolar hard sphere fluid

Lorenzo Rovigatti,[1] Sofia Kantorovich,[1,2,3] Alexey O. Ivanov,[3] José Maria Tavares,[4,5] and Francesco Sciortino[1,6]

[1]*Dipartimento di Fisica, Sapienza Università di Roma, Piazzale A. Moro 2, 00185 Roma, Italy*
[2]*University of Vienna, Boltzmanstrasse 5, 1090 Wien, Austria*
[3]*Ural Federal University, Lenin av. 51, 620083, Ekaterinburg, Russia*
[4]*Instituto Superior de Engenharia de Lisboa - ISEL, Rua Conselheiro Emídio Navarro 1, P-1950-062 Lisbon, Portugal*
[5]*Centro de Física Teórica e Computacional, Avenida Professor Gama Pinto 2, P-1649-003 Lisbon, Portugal*
[6]*CNR-ISC, Sapienza Università di Roma, Piazzale A. Moro 2, 00185 Roma, Italy*

(Received 26 June 2013; accepted 9 September 2013; published online 1 October 2013)

In this contribution, we investigate the low-temperature, low-density behaviour of dipolar hard-sphere (DHS) particles, i.e., hard spheres with dipoles embedded in their centre. We aim at describing the DHS fluid in terms of a network of chains and rings (the fundamental clusters) held together by branching points (defects) of different nature. We first introduce a systematic way of classifying inter-cluster connections according to their topology, and then employ this classification to analyse the geometric and thermodynamic properties of each class of defects, as extracted from state-of-the-art equilibrium Monte Carlo simulations. By computing the average density and energetic cost of each defect class, we find that the relevant contribution to inter-cluster interactions is indeed provided by (rare) three-way junctions and by four-way junctions arising from parallel or anti-parallel locally linear aggregates. All other (numerous) defects are either intra-cluster or associated to low cluster-cluster interaction energies, suggesting that these defects do not play a significant part in the thermodynamic description of the self-assembly processes of dipolar hard spheres.
© *2013 AIP Publishing LLC*. [http://dx.doi.org/10.1063/1.4821935]

I. INTRODUCTION

Dipole-dipole interactions are extremely common in nature, and they play a very important role in determining the phase behaviour of many substances, ranging from water[1,2] to protein solutions.[3] Colloids interacting through strong dipolar interactions, the so-called ferrofluids, are a technologically relevant class of liquids with plenty of applications, ranging from heat transfer to friction-reduction.[4] Despite the extensive investigations,[5–10] it is still unclear whether purely dipolar interactions are able to sustain a gas-liquid-like phase separation. Early theoretical and numerical studies suggested the existence of a critical point[11,12] between a gas and a liquid phase. Simulation studies of systems which have the dipolar hard sphere (DHS) fluid as a limiting case have provided estimates of the critical point location by extrapolating the values of the computed critical parameters as the investigated system tends to the DHS one.[13–15] Direct simulation of the DHS model are indeed rather difficult, requiring optimisation of the numerical procedure to reach equilibrium in the region of temperatures where the critical phenomenon is supposed to be located. Different from standard liquids, at low temperature, DHS self-assemble into head-to-tail flexible chains, giving rise to a self-assembly process that competes with the standard gas-liquid phase separation.[15–18] Very recent simulations,[18] with algorithms explicitly designed to efficiently relax the strong head-to-tail interactions, have been able to explore the region in which the critical point was supposed to be located without finding evidence of critical behaviour. Theoretical predictions have also been rather contradicting. Theories from the mid-1990s, accounting for chain formation, backed up the claim of the absence of a critical point.[19,20] By contrast, a recent thermodynamic perturbation theory, which also accounts for the chaining, predicts the existence of a critical point.[21]

At low temperature T and density ρ, dipolar particles tend to form chain-like structures,[16,22] giving rise to a fluid made up of long, transient, and weakly interacting chains (structures in which all particles, except two, have two neighbours aligned in the nose-to-tail configurations) and rings (structures in which all particles are doubly bonded).[18,23,24] As the density increases, inter-cluster interactions start to rise and, eventually, chains and rings merge together to form branched clusters[25–28] via the emergence of junctions, i.e., of particles which have more than two neighbours. The analysis of equilibrium configurations confirms that, for any reasonable criterion for classifying two neighbour particles as bonded, a significant number of branching points exists,[15,18] providing a mechanism for connecting chains and rings in a percolating three-dimensional network. One of the most elegant theoretical approaches[29] attempting to describe the phase behaviour of DHS was indeed based on the competition between two different groups of network defects: three-way junctions (TWJ) and chain ends (CE). Under some specific conditions, the mean-field theory developed by Tlusty and Safran[29] (TS) predicts a phase transition between a low-density, CE-rich phase and a high-density, TWJ-rich phase. If the ratio r between the energies associated with these two classes of defects lies within the range [1/3, 1/2], the resulting phase diagram is

 © 2013 AIP Publishing LLC

Downloaded 01 Oct 2013 to 141.108.6.119. This article is copyrighted as indicated in the abstract. Reuse of AIP content is subject to the terms at: http://jcp.aip.org/about/rights_and_permissions

reentrant, that is, the density of the coexisting liquid branch decreases as the system is cooled down. If $r < 1/3$, the theory predicts no phase separation.

To simplify the complexity of the DHS interactions and elucidate more the competition between chaining and branching, primitive models of patchy colloids have been designed and investigated theoretically via the Wertheim theory and numerically via Monte Carlo (MC) methods.[30,31] Both the parameter free Wertheim theory and the MC simulations have confirmed the mean field predictions of the TS theory. These studies have highlighted the delicate balance between branching and chaining energies, as well as the relevant role of the bonding volumes in controlling the temperature scale of the transition, offering interesting clues on possible extensions of the TS approach.[32,33] A close comparison between patchy models and DHS requires a mapping between chaining and branching energies as well as their associated volume of bonding. In this contribution, we critically scrutinise Monte Carlo configurations of DHS at low temperatures and low-to-intermediate densities, with the aim of quantifying the elementary clusters of the fluid and their inter-cluster interactions. We focus on all particles with more than two bonded neighbours and attempt to classify their local topology in order to provide an exhaustive description of the branching points and of their role in mediating the interactions between the elementary clusters, i.e., chains and rings. We present the analysis of the density and temperature dependence of their number, as well as an estimate of the energetic cost associated to their formation, which will help improving the comparison with primitive models. Despite the very large number of found branching topologies, we discover that the TWJ junctions, the ones specifically included in the TS mean field approach,[34] are the strongest mediators of the inter-cluster interactions but their number is rather limited, decreases on cooling, and it is not sufficient to generate a percolating interconnected network. On lowering T, the interactions between (anti-)parallel locally linear structures (chain-chain, ring-ring, chain-ring) — despite their higher energy — become more relevant. Different from TWJ, the formation of these four-way junctions does not require any change in the concentration of chain ends.

II. MODEL

The pair interaction energy between two DHS particles i and j is given by

$$u(i,j) = u_{HS}(r_{ij}) + \frac{\boldsymbol{\mu}_i \cdot \boldsymbol{\mu}_j - 3(\boldsymbol{\mu}_i \cdot \hat{\mathbf{r}}_{ij})(\boldsymbol{\mu}_j \cdot \hat{\mathbf{r}}_{ij})}{r_{ij}^3}, \quad (1)$$

where u_{HS} is the hard-sphere potential between particles of diameter σ, $\boldsymbol{\mu}_i$ is the dipole moment of particle i, $\mathbf{r}_{ij}$ is the vector joining the centres of i and j, and r_{ij} is its length. The DHS pair potential exhibits two minima for $r_{ij} = \sigma$: in the lowest energy configuration, of depth $2\mu^2/\sigma^3$, the two particles are in contact, with their dipoles oriented in a nose-to-tail configuration. The secondary minimum, of depth μ^2/σ^3, is given by two particles being side-by-side and having their dipoles oriented in an anti-parallel fashion. The former leads to the characteristic formation of linear structures, whereas the latter, at low temperatures, is responsible for the weak interaction acting between nearby chain-like structures.

In the following, $k_B = 1$, lengths are presented in units of σ, energies and temperatures are given in units of μ/σ^3.

III. METHODS

In this work, we analyse equilibrium configurations generated via Monte Carlo simulations[18,26] of the DHS fluid in the NVT ensemble. Aggregation-volume-bias MC moves,[35] specifically adapted for the DHS model, had been implemented to facilitate breaking and reforming of the strong head-to-tail bonds.[26] Long range interactions were taken into account using Ewald sums with conducting boundary conditions.[36] We analyze simulations at $T = 0.125$, 0.140, 0.155, 0.170, 0.250, 0.50 and in the density range $\rho \in [0, 0.14]$. The total number of particles in the system is $N = 5000$.

As previously done in Refs. 18 and 26, two particles i and j are defined as bonded if their mutual distance r_{ij} is less than $r_c = 1.3\sigma$ and if their pair interaction energy is negative. The value of r_c coincides with the first minimum of the radial distribution function. Particles with more than two bonded neighbours are considered as defects. Defect particles are coloured in orange in the simulation snapshots shown throughout this work, while particles with one or two neighbours are coloured in green. We also perform cluster analyses on the configurations and classify clusters according to their topology:

- Clusters containing only doubly bonded particles are labelled as rings.
- Monomers or clusters containing two singly bonded particles and only doubly bonded particles are labelled as chains.
- Every other cluster (i.e., every structure containing at least a defect) is called a branched structure.

In the following, we will refer to single defective particles (i.e., particles with more than two bonded neighbours) as defects or defect particles. A set of neighbouring defect particles will be referred to as a defect cluster or junction.

IV. RESULTS

A. Identification of the defect clusters and their spatial correlation

The density and temperature dependence of the number of defects has been previously investigated[18] but no attempt has been made in scrutinising the geometry of the defect and of its nearby particles to reveal different geometrical and/or topological patterns. Here, we attempt to classify these defects into different categories, depending on the local connectivity properties. To this aim, we start by grouping defects into clusters of defects, based on a proximity criterion. We assume that two defects belong to the same cluster if their mutual distance is less than 1.5σ. A standard cluster algorithm is then run to identify all possible independent clusters of defects and

Downloaded 01 Oct 2013 to 141.108.6.119. This article is copyrighted as indicated in the abstract. Reuse of AIP content is subject to the terms at: http://jcp.aip.org/about/rights_and_permissions

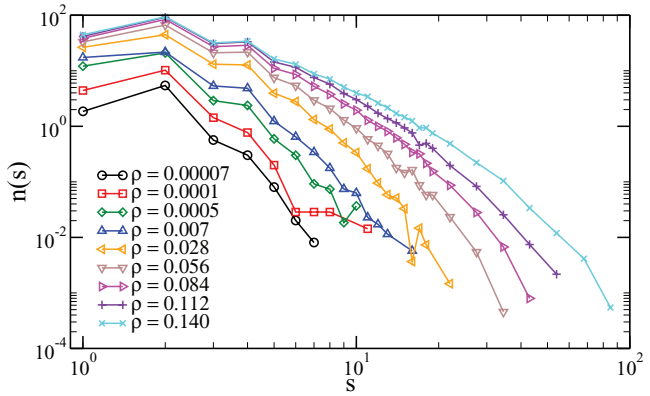

FIG. 1. Defect cluster size distributions for $T = 0.140$ at all investigated densities.

their relative size. Of course, particles with two or less bonded neighbours do not enter in the cluster analysis.

The resulting distribution $n(s)$ of the different defect cluster sizes s, normalised such that $\sum_s sn(s)$ is the total number of defect particles, is shown in Figure 1 (ρ-effect) and Figure 2 (T-effect).

The first thing we note in Figure 1 is that all curves are non-monotonic and have a peak at $s = 2$, and grow upon increasing density. In addition, there is a shoulder at $s = 4$ that eventually evolves into a peak as the density increases. The effect of density is monotonic: as ρ increases there are more and more defect clusters of any given size s.

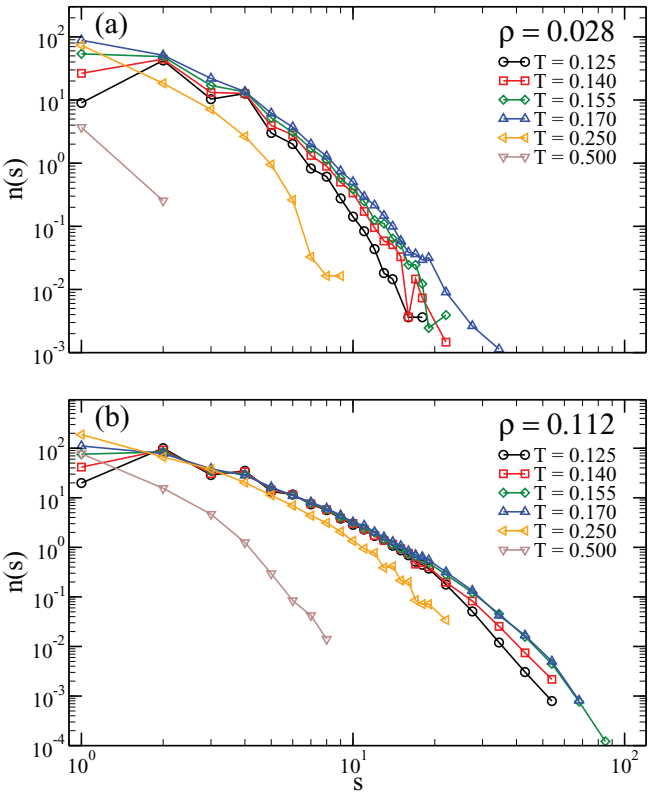

FIG. 2. Defect cluster size distributions at (a) $\rho = 0.028$ and (b) $\rho = 0.112$ for all investigated T.

Figure 2 shows the defect cluster size distributions at fixed densities and different temperatures. For the densities investigated in this work and at high temperatures, $T \geq 0.5$, the DHS fluid is made up of basically non-interacting particles. As the system is cooled down, $0.5 \geq T \geq 0.2$, particles start to self-assemble into small, disordered clusters.[37] At this T, thermal fluctuations are so relevant that the formed clusters do not have a clear chain-like shape and contain many defects. In this regime, defect cluster size distributions are monotonic and do not have any of the features found at low temperatures. As T is further lowered, $T < 0.2$, the DHS fluid enters in the proper self-assembly region and it is made of persistent chain-like clusters which, depending on density, are more or less connected together by branching points.[19,20,26] For $T < 0.2$, the number of $s = 1$ defect clusters decreases with T and the curves have a non-monotonic behaviour. We ascribe the qualitative difference between defect cluster size distributions at temperatures higher and lower than $T = 0.2$ to the onset of the chaining process. The non-monotonicity of the curves stems from the different T-dependence of defect clusters of different sizes, as discussed later on. Interestingly, the number of defect clusters of size 2 and 4 has a weak temperature dependence for $\rho > 0.007$. For $\rho \geq 0.112$, the whole distribution of defect clusters having $1 < s \lesssim 20$ does not evolve with T. This is another evidence of the lack of change in the structure of these low-T, intermediate-density systems.[26]

B. Classification

The defect cluster size distributions reveal that the most numerous clusters of defects are composed by a small number of defect particles, with a preference towards even numbers. Furthermore, a visual inspection of the configurations suggests that defect clusters share some common features that we decide to exploit to properly classify the structure of the fluid. In addition, we notice that large aggregates of defects can be resolved as combination of clusters of smaller defects.

To categorise the defect clusters, we assign two integer numbers, s and w, to each defect cluster: s is the number of defects composing the defect cluster (i.e., its size) and w is the number of chain-like segments departing from it (number of ways out). The latter is calculated by counting the number of distinct particles that are bonded neighbours of the particles in the defect clusters and but are not members of it, as shown in the following figures. Note that, by this definition, a particle having two neighbours, both of which are part of the same defect cluster, is not a way out and therefore it does not contribute to the value of w. The T- and ρ-dependence on the number of defect clusters for different s and w is analysed in Sec. IV C.

Defect clusters of size one ($s = 1$) are always characterised by $w = 3$. Figure 3(a) shows two typical examples of these structures. The $s = 1$, $w = 3$ defect clusters are Safran defects (TWJs), i.e., the class of defects which have been considered the key structures (together with the chains, but neglecting the rings) in controlling the thermodynamic behaviour of dipolar fluids in general and dipolar hard-spheres in particular.[34]

Downloaded 01 Oct 2013 to 141.108.6.119. This article is copyrighted as indicated in the abstract. Reuse of AIP content is subject to the terms at: http://jcp.aip.org/about/rights_and_permissions

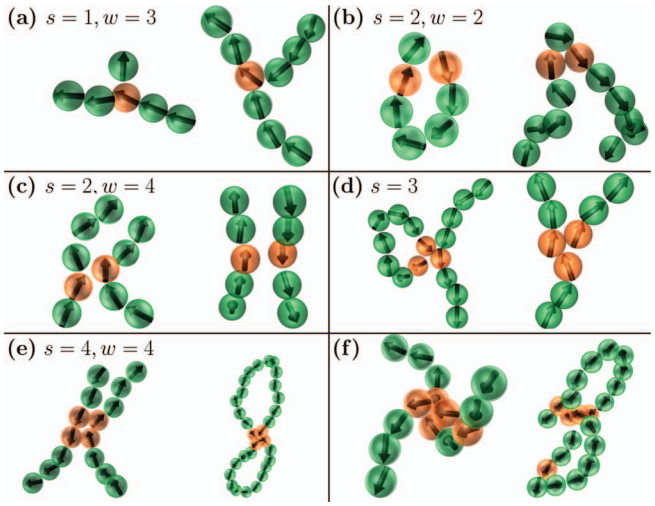

FIG. 3. (a) Two $s = 1$, $w = 3$ defect clusters. (b) $s = 2$, $w = 2$ defect clusters. This kind of defect clusters stems from intra-cluster interactions. (c) $s = 2$, $w = 4$ defect clusters. These form when two linear structures are close to each other. The result is a weak inter-cluster interaction. (d) $s = 3$ defect clusters with $w = 4$ (left) and $w = 3$ (right). The right defect cluster is a slightly defective TWJ. The one on the left is similar in nature to the defect clusters having both s and w as even numbers. (e) $s = 4$, $w = 4$ defect clusters. These originate from the interaction between chains, rings, or part of chain-like structures. (f) Defect clusters with a mixed nature. (Left) A $s = 5$, $w = 3$ defect cluster which can be seen as a combination of an intra-cluster defect and a TWJ. (Right) A $s = 4$, $w = 5$ defect cluster coming from a $s = 4$, $w = 4$ defect cluster and a $s = 2$, $w = 2$ defect cluster.

Defect clusters with $s = 2$ can be divided into two main categories: defect clusters having $w = 2$ (Figure 3(b)) and defect clusters having $w = 4$ (Figure 3(c)). As shown in Figure 3(b), the former originate from intra-cluster interactions (or equivalently from the thermal distortion of the cluster) and, as such, possibly do not play a significant role. By contrast, $s = 2$, $w = 4$ defect clusters, shown in Figure 3(c), are related to inter-cluster interactions. They form when two linear-like structures (e.g., a chain, a ring, or a part thereof) are close enough.

The majority of the defect clusters having $s = 3$ has either $w = 3$ or $w = 4$. Figure 3(d) provides two examples of these structures. They have the same nature of defect clusters with $s = 1$, $w = 3$ (Safran-like defects) and $s = 2$, $w = 4$ (chain-ring interaction), respectively.

The most numerous defect clusters with $s = 4$ are those with $w = 4$. Two examples are shown in Figure 3(e). Similar to the ($s = 2$, $w = 4$) and ($s = 3$, $w = 4$) cases, these defect clusters stem from the interaction between chains, rings, or part of chain-like structures.

Every other observed defect cluster is just a combination of the aforementioned defect clusters. We provide two examples in Figure 3(f). The left panel contains a "defective" ring touching a chain. It is a four-way junction ($s = 3$, $w = 4$) plus two intra-cluster defects. In the right panel, two rings are joined together by a four-way junction ($s = 4$, $w = 4$). An additional monomer makes it a five-way junction.

To summarise, despite the large number of possibilities, two main classes are found: defect clusters with $w = 3$ that, independently from the value of s, are TWJs and can always be associated with chain branching. By contrast, defect clusters with $w = 2$ or $w = 4$, regardless of s, are responsible for intra-cluster interactions and interactions between rings or chains, respectively. Therefore, both defect classes do not involve bonding of loose chain ends.

C. Density and *T* dependence of the concentration of defects

Next, we investigate the ρ- and T-dependences of the density of defect clusters, according to their type.

Figure 4 shows the density of defect clusters ρ_d for the four most common sizes s as a function of density for two temperatures. In all cases, there seems to be a density range for which all ρ_d are compatible with power-laws with similar exponents. As previously noted, at low temperature the number of defect clusters with $s = 2$ is larger than the number of defect clusters with $s = 1$ for all densities. This is due to the decrease in the number of $s = 1$ defect clusters occurring upon cooling, the physical origin of which will be discussed at the end of this section.

Figure 5 shows ρ_d as a function of density for defect clusters having $1 < s < 5$, accounting also for the different values of w, i.e., the number of ways out of the junction. Since every $s = 1$ defect cluster has $w = 3$, we omit this class of junctions from this specific analysis. From the plots it is clear that, for $\rho > 0.01$, the most abundant defect clusters having $s > 1$ also have $w = 4$. Among $s = 3$ defects there is also a non-negligible number of three-way junctions.

The previous analysis confirms that defect clusters should be classified according to w and that only junctions having

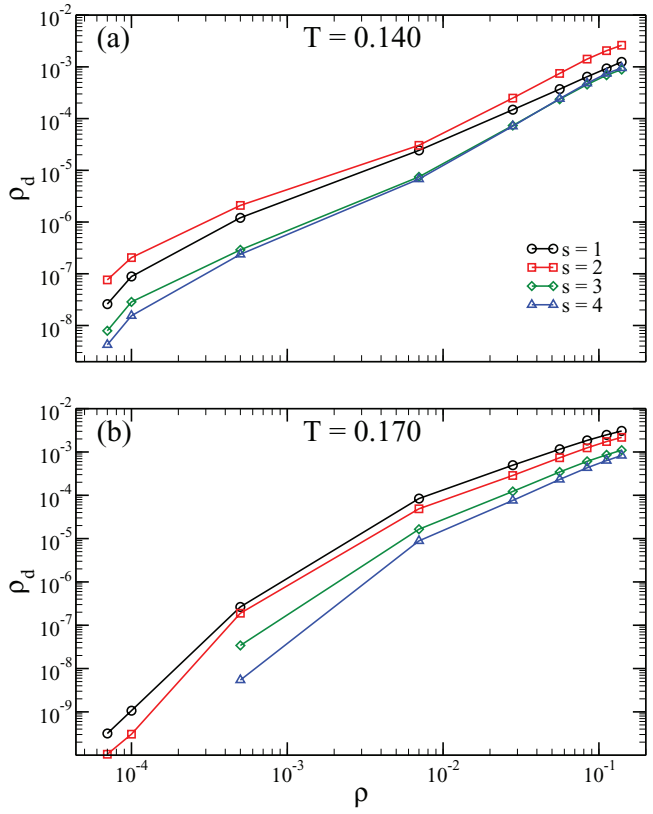

FIG. 4. Density of defect clusters having $s = 1, 2, 3, 4$ for (a) $T = 0.140$ and (b) $T = 0.170$ as a function of the overall density.

Downloaded 01 Oct 2013 to 141.108.6.119. This article is copyrighted as indicated in the abstract. Reuse of AIP content is subject to the terms at: http://jcp.aip.org/about/rights_and_permissions

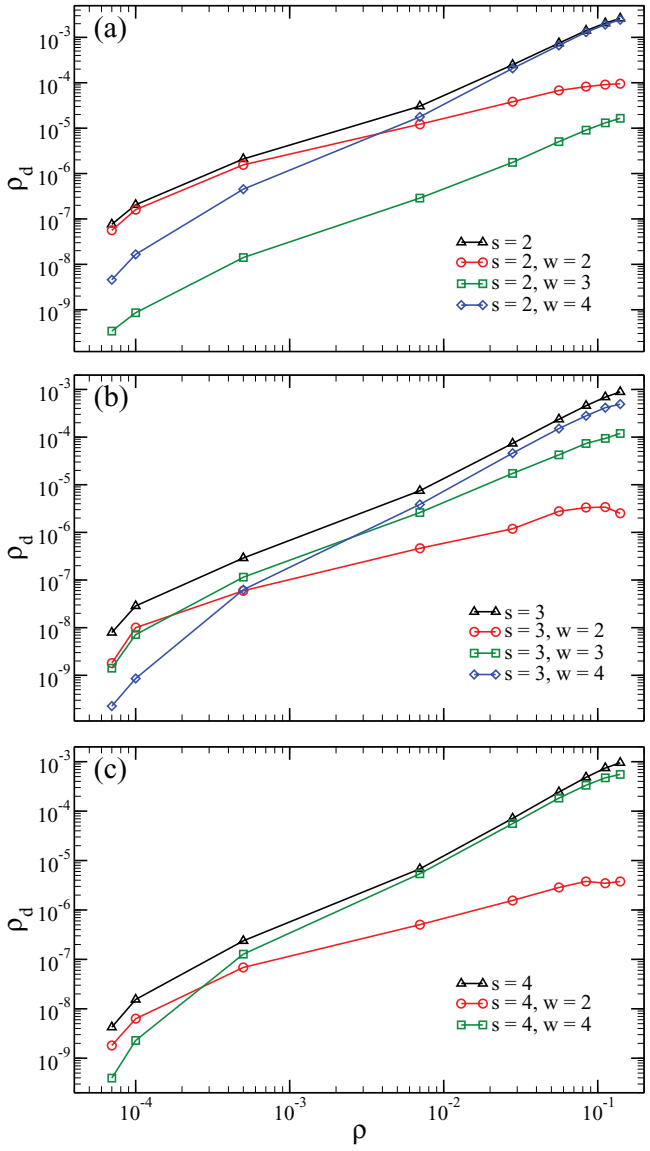

FIG. 5. Density of defect clusters as a function of the overall density for $T = 0.140$. We further classify defect clusters by counting the number of ways out of each junction w. (a) Defect clusters with $s = 2$. (b) Defect clusters with $s = 3$. (c) Defect clusters with $s = 4$.

$w = 3$ and $w = 4$ originate from inter-cluster interactions. To further investigate the role of these classes of defects in the DHS fluid, we compute their density as a function of ρ at the lowest investigated T. The results are shown in Figure 6. The density of TWJs increases with ρ but decreases as the system is cooled. Since the TWJ defect arises from the interaction of a chain-end and a linear structure [see Fig. 3(a)], its statistical relevance depends on the concentration of chain ends. The latter are characterised by a significant energetic cost (since they could associate in head-to-tail configurations) and, hence, are more and more unfavourable as T goes down. This explains the observed decrease of the number of TWJs with T. We also note that for $\rho > 0.01$, the increase in density is consistent with a power-law behaviour with an exponent which depends slightly on T but tends, as T decreases, to the value 3/2 predicted by the TS theory. We note that the total number of $w = 3$ defect clusters (inset of Fig. 6) is very small if

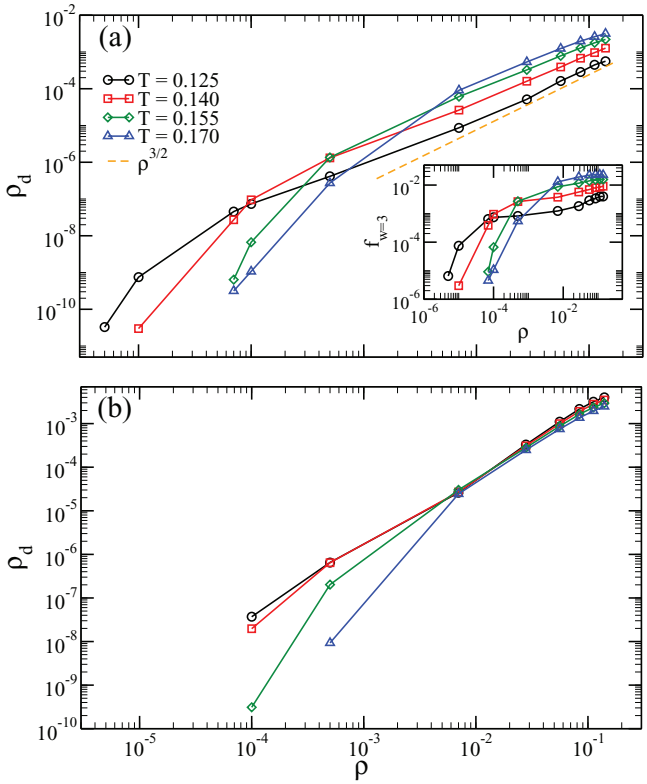

FIG. 6. Density of defect clusters having (a) $w = 3$ and (b) $w = 4$ as a function of the overall density for different temperatures. The orange dashed line in (a) is the predicted power-law behaviour for the density of TWJs.[29] Inset of panel (a): the number of three-way junctions over the total particle number N.

compared to the number of particles in the system. Indeed, at the lowest temperature and highest density, there are no more than 20 three-way junctions in a system composed of 5000 particles.

Defect clusters having $w = 4$ behave in a substantially different way. Indeed, if T decreases, the density of these junctions grows, albeit rather slowly, for $\rho > 0.01$. Such an increase upon cooling suggests that $w = 4$ defect clusters are energetically stabilised. Indeed, different from TWJ, $w = 4$ defect clusters [see Fig. 3(e)] intervene in cluster-cluster interactions which do not involve chain ends. A thermodynamic description aiming at predicting the low T DHS phase behaviour has to take into account also this class of defects.

D. Defect energy

We next focus on the energetic cost of creating a defect. We consider the system to be composed of chains and rings, and calculate the interaction energy associated to the defect formation.

We operatively define the energy associated with a defect cluster c with given s and w, $\epsilon_{s,w}$, as the interaction energy between the two clusters (either a ring or a chain) which are joined together by c. In order to compute $\epsilon_{s,w}$, we first remove all branching points by assigning to each particle a maximum of two neighbours. In this way, only chains and rings remain in the system. To do so in an umbiguous way, we first make a list of all bonded pairs and sort it in ascending order according to their mutual interaction energy, from the strongest

Downloaded 01 Oct 2013 to 141.108.6.119. This article is copyrighted as indicated in the abstract. Reuse of AIP content is subject to the terms at: http://jcp.aip.org/about/rights_and_permissions

bonds to the weakest ones. Then, we go through the sorted list, starting from the most energetic pair and classify the selected pair interaction as a bond participating in a chain or in a ring if and only if none of the two particles involved in the bond have already two bonds formed. As a result of the procedure, all particles in the system have at most two bonds. Under these conditions, the system is composed by construction of only chains and rings. In the following, we call this procedure "removal of the branching points." This process allows us to quickly separate defects that are intra-cluster (and hence neglected in the following, being thermal distortions of the chains or of the rings) and defects that connect distinct chains and/or rings. More specifically, we loop over all inter-clusters defects and we compute the energy associated with each defect cluster c, after classifying it according to its s and w. For each c, we identify the n clusters $c_1, c_2, \ldots$ involved in the formation of c and assign to c an energy given by

$$\epsilon^c_{s,w} = \frac{1}{2}\sum_{i=1}^{n}\sum_{j=1}^{n} u_{\text{cluster}}(c_i, c_j), \tag{2}$$

where

$$u_{\text{cluster}}(c_i, c_j) = \sum_{p\in c_i}\sum_{q\in c_j} u(p, q), \tag{3}$$

where $u(p, q)$ is the interaction energy between particles p and q as given by Eq. (1).

We note that, by construction, this procedure computes the energy of all inter-clusters defects, disregarding completely intra-clusters defects. Interestingly, all $s = 2$, $w = 2$ defect clusters, such as those shown in Figure 3(b), fall into the latter category. Since we analyse defect clusters having up to $w = 4$, the employed procedure involves at most two clusters. For clarity, Figure 7 shows how the described algorithm works. We note on passing that for the investigated classes ($s = 1$, $w = 3$, $s = 3$, $w = 3$, $s = 2$, $w = 4$, and $s = 4$, $w = 4$) the fraction of inter-cluster defect clusters, defined as the number of inter-cluster junctions of a certain type over the total number of junctions of the same type, increases with density and it is always larger than 80% for $\rho > 0.06$.

Next, we compute the distribution probability $P(\epsilon_{s,w})$ for the energy associated to the most common defect clusters. Figure 8 shows the results for $T = 0.140$ and $\rho = 0.007$. All the distributions feature a peak and a long tail extending at very low energies. The position of the peaks indicates that $w = 3$ defect clusters are usually associated to lower energies than $w = 4$ junctions. We note that $s = 3$, $w = 3$ defect clusters have a lower average energy than any other defect clusters, but they are almost an order of magnitude less abundant than $s = 1$, $w = 3$ junctions, as shown in Figs. 4(a) and 5(b).

The TS theory associates an energetic cost with the formation of a CE (ϵ_1^{TS}) and with the formation of a TWJ (ϵ_3^{TS}). These values are calculated assuming as a reference the energy of a head-to-tail bond e_b. Since breaking a head-to-tail bond costs e_b but produces two CEs, then $\epsilon_1^{TS} = e_b/2$. Similarly, once a chain-end joins a chain to form a TWJ, gaining what we have called $-\epsilon_{1,3}$, the corresponding value for ϵ_3^{TS} is $-\epsilon_{1,3} + \epsilon_b/2$. In the TS picture, both ϵ_1^{TS} and ϵ_3^{TS} are independent of temperature and density. Figure 9(a) shows $P(\epsilon_{1,3})$

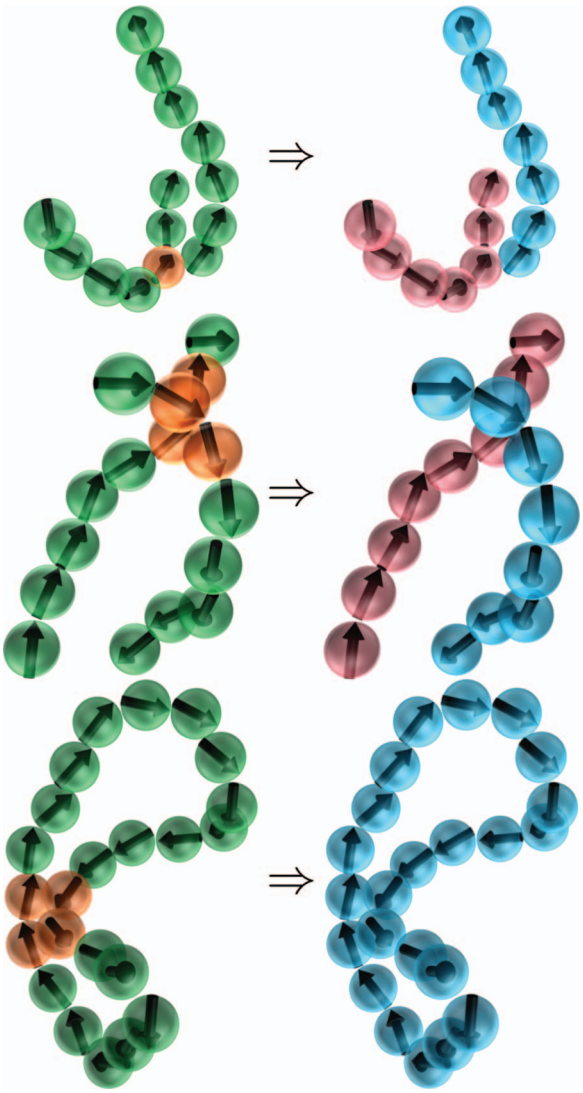

FIG. 7. Effect of the removal of branching points. (Top) A TWJ ($s = 1$, $w = 3$) made up of two chains which are revealed by the removal procedure. (Middle) The interaction between two chains results in a cluster containing a $s = 4$, $w = 4$ defect cluster. The removal procedure splits the original cluster into two separated chains. (Bottom) An intra-cluster interaction generates a $s = 4$, $w = 4$ defect cluster whose removal results in the identification of the original cluster as a ring.

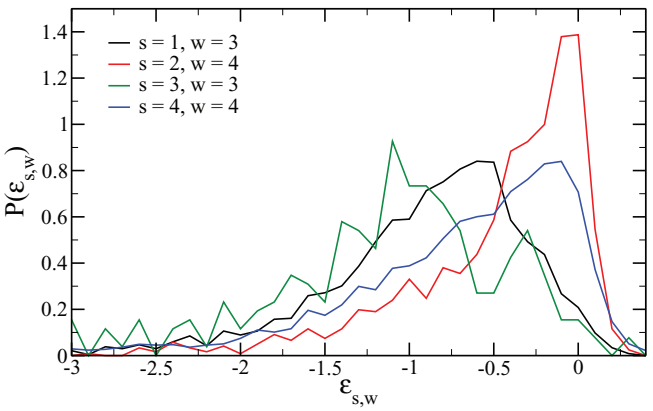

FIG. 8. Distribution probability $P(\epsilon_{s,w})$ for $T = 0.140$ and $\rho = 0.007$.

Downloaded 01 Oct 2013 to 141.108.6.119. This article is copyrighted as indicated in the abstract. Reuse of AIP content is subject to the terms at: http://jcp.aip.org/about/rights_and_permissions

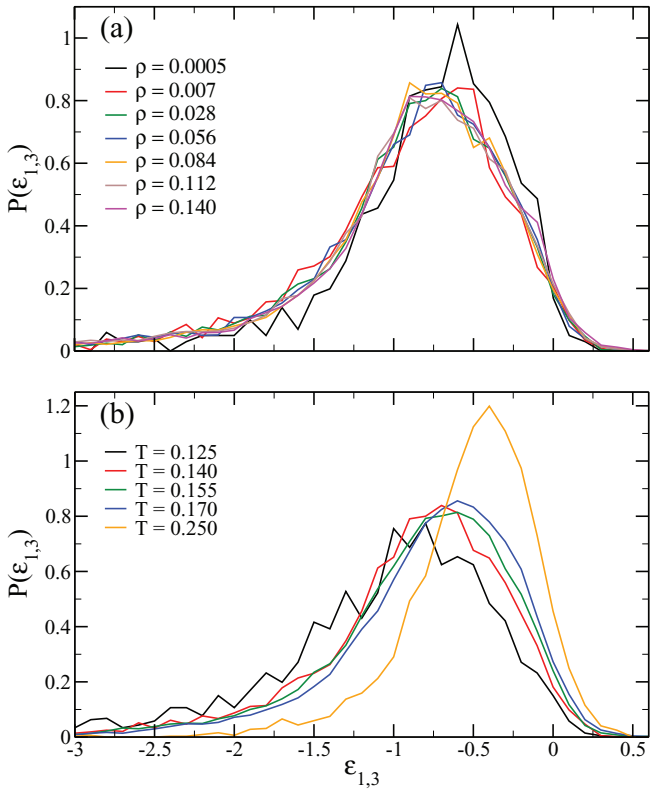

FIG. 9. (a) Distribution probability $P(\epsilon_{1,3})$ for $T = 0.140$ at different densities. (b) Distribution probability $P(\epsilon_{1,3})$ at $\rho = 0.007$ for different T.

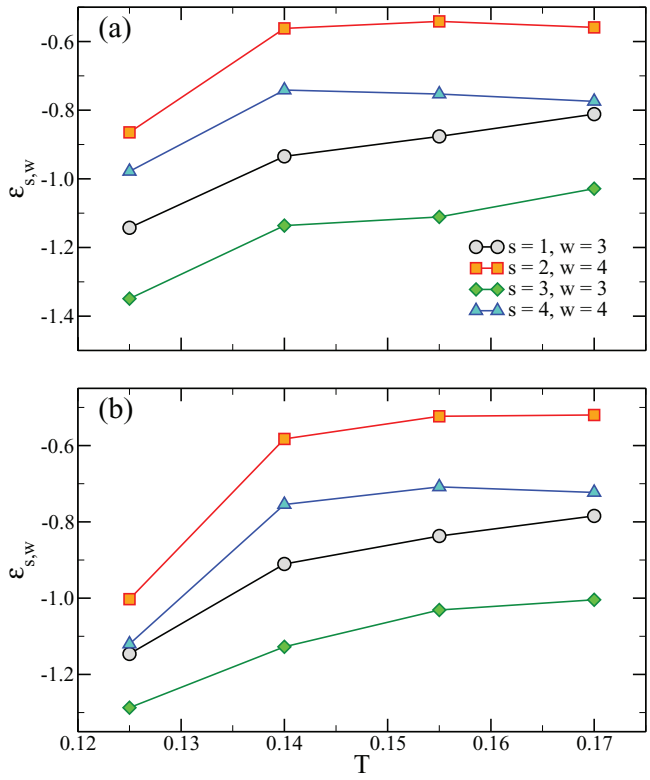

FIG. 10. Average $\epsilon_{s,w}$ at (a) $\rho = 0.028$ and (b) $\rho = 0.140$ for different T.

at fixed $T = 0.140$ and different densities. It is clear that, at least for $\rho > 0.0005$, $\epsilon_{1,3}$ is density-independent, as assumed by TS.

Figure 9(b) shows the temperature dependence of $P(\epsilon_{1,3})$. At the highest T, the distribution has a sharp peak at rather high energies, ≈ -0.4. As T decreases, the peak moves to lower energies, while the distribution widens and extends to rather low energies (down to -5, not shown). This residual T dependence is expected, in light of the different volume explored by bonded particles at different temperatures. A qualitatively similar dependence on ρ and T is also observed for $P(\epsilon_{4,4})$ (not shown).

Figure 10 shows $\epsilon_{s,w}$ averaged over all defect clusters having the same s, w values for the four most common defect classes as a function of T and for two different densities. As assumed by the TS theory, three-way junctions are the most energetically favourable class of branching points. Quite unexpectedly, also $s = 4$, $w = 4$ defects are associated to low energies and, at the lowest T and for high densities, $\epsilon_{1,3}$ and $\epsilon_{4,4}$ have comparable values. It is interesting to note that all curves bend downwards significantly below $T \approx 0.140$, suggesting that at this low T, some sort of structural change occurs in the local geometry of defect clusters. An inherent structure analysis[38] could perhaps shed light on this phenomenon.

E. Rings and chains size distributions without branching points

The removal procedure introduced in Sec. IV D provides an unambiguous way of partitioning all the particles in chains and rings only (monomers are considered as chains of length one). The structure of the system with all the branching points removed can then be analysed by computing cluster size distributions.

Figure 11(a) shows the number of clusters (chains or rings) $n(s)$ of size s found in the system for a fixed $T = 0.140$ and different densities. At low densities, these curves are similar to what is found without removing all the defects: both ring and chain size distributions extend to larger and larger sizes as ρ increases.[26] Often, clusters (especially chains) are significantly longer than the size of the simulation box, sometime going several times through the periodic boundary conditions. After a certain threshold density, which depends slightly on T, the number of rings rapidly diminishes and, quite surprisingly, chains begin to shorten. This non-monotonic behaviour can be clearly seen in Figure 11(b), which shows the average size $\langle s \rangle$ of rings and chains for all the studied low-T state points as the density is changed. Indeed, $\langle s \rangle$ exhibits a maximum in density for both chains and rings.[39] The average ring and chain sizes in a system of non-interacting clusters are monotonically increasing functions of ρ,[40] and therefore we ascribe the presence of the maxima to either finite size effects or to inter-cluster interactions.[41,42]

F. Percolation line

In previous studies, no distinction was made on the different nature of the defects. Assuming that all particles with more than two bonded neighbours are equally relevant (i.e., if all defects are assumed to contribute to connections between

Downloaded 01 Oct 2013 to 141.108.6.119. This article is copyrighted as indicated in the abstract. Reuse of AIP content is subject to the terms at: http://jcp.aip.org/about/rights_and_permissions

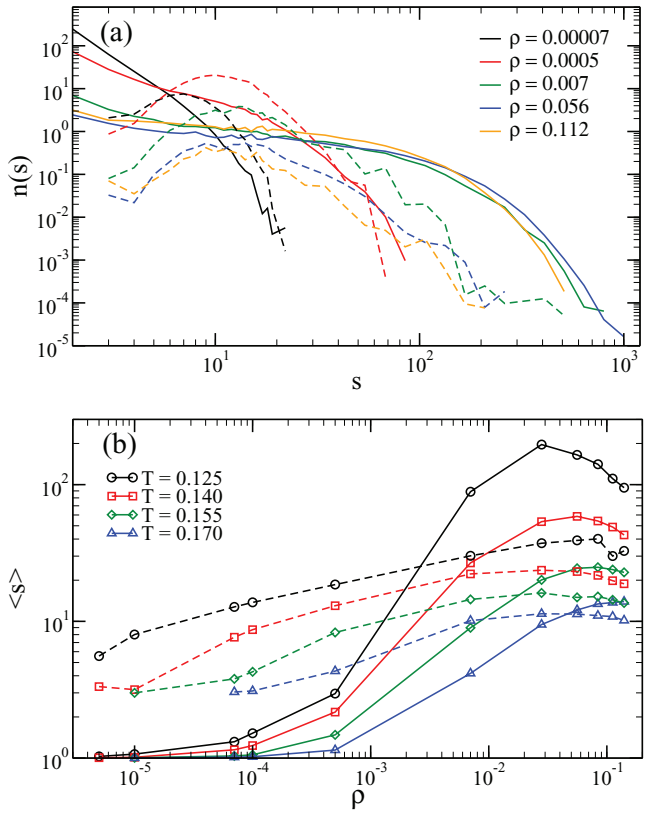

FIG. 11. (a) Cluster size distributions for chains (solid lines) and rings (dashed lines) for different densities and $T = 0.140$. (b) Average cluster size for chains (solid lines) and rings (dashed lines) as a function of density and for different T.

different chains and rings) percolation in DHS systems was found to occur at surprisingly low densities.[18,26] Since percolation is a prerequisite of criticality, the presence of strong clustering and percolation clashes with the absence of a critical point. Results shown in Secs. IV A–IV E strongly suggest that the only thermodynamically relevant inter-cluster interactions are those giving rise to $w = 3$ and $s = 4$, $w = 4$ defect clusters. It is thus relevant to re-examine the location of the percolation *locus* when only these types of defects are taken into account. This analysis can be carried out by removing all the branching points belonging to the other classes of defects. At the end of the removal procedure, the system contains only chains, rings, and clusters branched via three-way and four-way junctions. In order to compute the percolation line, we calculate the fraction of percolating configurations, i.e., the number of configurations containing a spanning cluster over the total number of configurations. To minimise the possibility of finite size effects, we leave out from the analysis all configurations in which, after the removal of all defects, a ring of infinite size (that is, a chain that closes via periodic boundary condition) was found, i.e., all the configurations that would be percolating even if the system were composed only by rings and chains.

Figure 12 shows the fraction of percolating configurations P_{perc}. Chains and rings are connected via either TWJ or $s = 4$, $w = 4$ defect clusters. A state point is regarded as percolating if more than 50% of its configurations contains a spanning cluster. At lower T, percolation takes place at smaller densities. At $T \gtrsim 0.17$, percolation is never observed in the explored density region. We also compute the percolation properties of the system in which chains and rings are connected only via TWJs (dashed lines in Fig. 12). In this case, percolation is suppressed and P_{perc} does not assume the typical sigmoidal shape. This may be ascribed to the small fraction of junctions present in the system (the fraction of TWJs is typically smaller than 2×10^{-2}, see inset of Fig. 6), enhancing finite size fluctuations. We note that, if all defects are taken into account, independently on their statistical relevance, the system always percolates at $\rho \gtrsim 0.05$ for $T \leq 0.170$[26] and the percolation locus has a very weak dependence on ρ. The new data presented here show that, by considering only TWJs and $s = 4$, $w = 4$ defect clusters, the percolation line moves to higher densities and lower T.

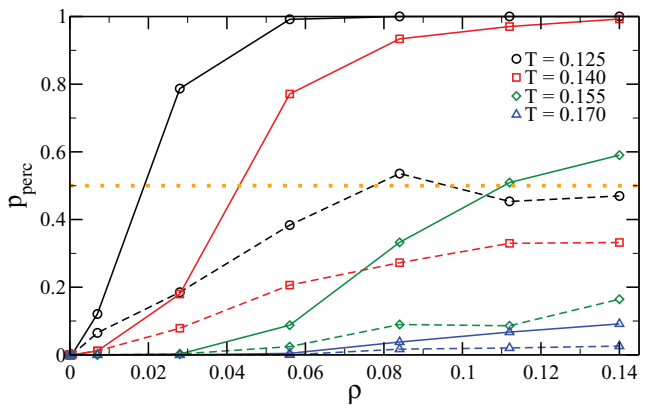

FIG. 12. Probability of finding a percolating configuration as a function of density for different T with all defects but TWJs and $s = 4$, $w = 4$ defect clusters removed (full lines). Dashed lines have been computed by considering TWJs only. Configurations containing percolating chains have been excluded from the analysis. State points are deemed as percolating if $P_{\text{perc}} > 0.5$ (orange dotted line).

V. CONCLUSIONS

We have presented a detailed study of the structure of defects in dipolar hard sphere systems. We have shown that defects cannot be considered as identical entities, as previously done, but need to be classified according to their local topology. We have proposed to categorise them according to their spacial proximity (s) and to the number of linear structures that come out from each defect (w). We have shown that this classification allows to distinguish the defects responsible for intra-cluster interaction, weak to intermediate inter-cluster interactions, and three-way junctions, the topology which was assumed to be relevant in the mean field theory of Tlusty and Safran.[34] To estimate the thermodynamic part of the defects, we have introduced a systematic procedure to identify and compute the energy associated with the formation of each class of defects, finding that only three-way junctions and $s = 4$, $w = 4$ defect clusters result in a non-negligible cluster-cluster attraction. Unlike TWJs, which are suppressed by chaining, $s = 4$, $w = 4$ junctions arise from the interaction between (anti-)parallel linear structures, and

Downloaded 01 Oct 2013 to 141.108.6.119. This article is copyrighted as indicated in the abstract. Reuse of AIP content is subject to the terms at: http://jcp.aip.org/about/rights_and_permissions

therefore these defect clusters do not induce a competition between ring- and chain-formation and branching.

This suggests that an extension of the TS theory should incorporate two important features: (i) it should include the previously neglected ring structures (whose role becomes dominant at low densities). Recent studies have shown that extensive ring formation in chaining and branching systems (i.e., adding ring formation to the TS approach) can result in a suppression of the phase separation process.[43,44] We also note that DHSs appear to be characterized by a scarcity of TWJs and by an abundance of rings, such that percolation through TWJs only is never observed. (ii) It should include $s = 4$, $w = 4$ defect clusters. These introduce a significant inter-cluster (ring-ring, chain-chain, and chain-ring) attraction, which appears to become relevant at low temperature. Including these interactions augments the connectivity of the system and favours percolation. Since gas-liquid criticality is commonly preceded by percolation,[45] a phase separation sustained by $s = 4$, $w = 4$ defect clusters, which are not suppressed by rings, could occur at low T. However, we note that it is possible to have percolation but not phase separation. This suggests that a patchy particle model for DHS, in which chaining and branching are modelled via dissimilar patches,[30] may require not only chain-chain or chain-branching interactions, but also an additional, weaker branching-branching contribution to mimic the $s = 4$, $w = 4$ defect clusters.

Finally, our study provides values for the energies associated with all the defect classes observed in the system. These values, together with a proper modelling of the topological connections along the lines of the TS theory and of the corresponding patchy particle models,[31] can be used to quantify the entropic cost associated to their formation. All in all, the data presented in this article will surely help in developing a theory able to model the long-sought low-T, low-ρ phase diagram of dipolar fluids.

ACKNOWLEDGMENTS

L.R., S.K., and F.S. acknowledge support from ERC-226207-PATCHYCOLLOIDS. A.O.I. acknowledges financial support from the Ministry of Education and Science of the Russian Federation under Project No. 2.609.2011. J.M.T. acknowledges financial support from the Portuguese Foundation for Science and Technology (FCT) under Contract Nos. PEstOE/FIS/UI0618/2011 and PTDC/FIS/098254/2008.

[1] J. K. Gregory, D. C. Clary, K. Liu, M. G. Brown, and R. J. Saykally, Science **275**, 814 (1997).
[2] P. L. Silvestrelli and M. Parrinello, Phys. Rev. Lett. **82**, 3308 (1999).
[3] F. W. Tavares, D. Bratko, A. Striolo, H. W. Blanch, and J. M. Prausnitz, J. Chem. Phys. **120**, 9859 (2004).
[4] R. E. Rosensweig, *Ferrohydrodynamics* (Courier Dover Publications, 1997).
[5] B. Groh and S. Dietrich, Phys. Rev. Lett. **79**, 749 (1997).
[6] I. Szalai and S. Dietrich, J. Phys.: Condens. Matter **20**, 204122 (2008).
[7] I. Szalai and S. Dietrich, Mol. Phys. **103**, 2873 (2005).
[8] C. Holm, A. Ivanov, S. Kantorovich, E. Pyanzina, and E. Reznikov, J. Phys.: Condens. Matter **18**, S2737 (2006).
[9] S. Kantorovich, J. Cerda, and C. Holm, Phys. Chem. Chem. Phys. **10**, 1883 (2008).
[10] P. J. Camp and G. N. Patey, Phys. Rev. E **62**, 5403 (2000).
[11] P. G. de Gennes and P. A. Pincus, Phys. Kondens. Mater. **11**, 189 (1970).
[12] K. Ng, J. P. Valleau, G. M. Torrie, and G. N. Patey, Mol. Phys. **38**, 781 (1979).
[13] N. G. Almarza, E. Lomba, C. Martín, and A. Gallardo, J. Chem. Phys. **129**, 234504 (2008).
[14] G. Ganzenmüller and P. J. Camp, J. Chem. Phys. **126**, 191104 (2007).
[15] G. Ganzenmüller, G. N. Patey, and P. J. Camp, Mol. Phys. **107**, 403 (2009).
[16] J. J. Weis and D. Levesque, Phys. Rev. Lett. **71**, 2729 (1993).
[17] J.-M. Caillol, J. Chem. Phys. **98**, 9835 (1993).
[18] L. Rovigatti, J. Russo, and F. Sciortino, Phys. Rev. Lett. **107**, 237801 (2011).
[19] R. van Roij, Phys. Rev. Lett. **76**, 3348 (1996).
[20] R. P. Sear, Phys. Rev. Lett. **76**, 2310 (1996).
[21] Y. V. Kalyuzhnyi, I. A. Protsykevytch, and P. T. Cummings, EPL **80**, 56002 (2007).
[22] A. Y. Zubarev and L. Y. Iskakova, Phys. Rev. E **61**, 5415 (2000).
[23] T. Prokopieva, V. Danilov, S. Kantorovich, and C. Holm, Phys. Rev. E **80**, 031404 (2009).
[24] S. Kantorovich, A. O. Ivanov, L. Rovigatti, J. M. Tavares, and F. Sciortino, Phys. Rev. Lett. **110**, 148306 (2013).
[25] R. Blaak, M. A. Miller, and J.-P. Hansen, Europhys. Lett. **78**, 26002 (2007).
[26] L. Rovigatti, J. Russo, and F. Sciortino, Soft Matter **8**, 6310 (2012).
[27] A. Zubarev and L. Iskakova, J. Exp. Theor. Phys. **116**, 286 (2013).
[28] P. D. Duncan and P. J. Camp, Phys. Rev. Lett. **97**, 107202 (2006).
[29] T. Tlusty and S. A. Safran, Science **290**, 1328 (2000).
[30] J. Russo, J. M. Tavares, P. I. C. Teixeira, M. M. Telo da Gama, and F. Sciortino, Phys. Rev. Lett. **106**, 085703 (2011).
[31] J. Russo, J. M. Tavares, P. I. C. Teixeira, M. M. Telo da Gama, and F. Sciortino, J. Chem. Phys. **135**, 034501 (2011).
[32] J. Tavares and P. Teixeira, Mol. Phys. **109**, 1077 (2011).
[33] N. G. Almarza, J. M. Tavares, E. G. Noya, and M. M. T. da Gama, J. Chem. Phys. **137**, 244902 (2012).
[34] A. Zilman, T. Tlusty, and S. A. Safran, J. Phys.: Condens. Matter **15**, S57 (2003).
[35] B. Chen and J. I. Siepmann, J. Phys. Chem. B **105**, 11275 (2001).
[36] B. Smith and D. Frenkel, *Understanding Molecular Simulations* (Academic, New York, 1996).
[37] E. A. Elfimova, A. O. Ivanov, and P. J. Camp, Phys. Rev. E **86**, 021126 (2012).
[38] T. A. Weber and F. H. Stillinger, J. Chem. Phys. **87**, 3252 (1987).
[39] Z. Wang, C. Holm, and H. W. Müller, Phys. Rev. E **66**, 021405 (2002).
[40] J. M. Tavares, L. Rovigatti, and F. Sciortino, J. Chem. Phys. **137**, 044901 (2012).
[41] A. Y. Zubarev and L. Y. Iskakova, Phys. Rev. E **65**, 061406 (2002).
[42] L. Y. Iskakova and A. Y. Zubarev, Phys. Rev. E **66**, 041405 (2002).
[43] N. G. Almarza, Phys. Rev. E **86**, 030101(R) (2012).
[44] L. Rovigatti, J. M. Tavares, and F. Sciortino, e-print arXiv:1309.5225.
[45] A. F. A. Coniglio, U. De Angelis, and G. Lauro, J. Phys. A **10**, 219 (1977).

Downloaded 01 Oct 2013 to 141.108.6.119. This article is copyrighted as indicated in the abstract. Reuse of AIP content is subject to the terms at: http://jcp.aip.org/about/rights_and_permissions